Specificity for the Exchange of Phospholipids Through Polymyxin B Mediated Intermembrane Molecular Contacts†

Yolanda Cajal,*,‡ Jiothy Ghanta,‡,§ Kalpathy Easwaran,§ Avadhesha Surolia,§ and Mahendra Kumar Jain*,‡

Department of Chemistry and Biochemistry, University of Delaware, Newark, Delaware 19716

Received November 13, 1995; Revised Manuscript Received March 7, 1996⊗

ABSTRACT: Structural specificity for the direct vesicle−vesicle exchange of phospholipids through stable molecular contacts formed by the antibiotic polymyxin B (PxB) is characterized by kinetic and spectroscopic methods. As shown elsewhere [Cajal, Y., Rogers, J., Berg, O. G., & Jain, M. K. (1996) *Biochemistry 35*, 299−308], intermembrane molecular contacts between anionic vesicles are formed by a small number of PxB molecules, which suggests that a stoichiometric complex may be responsible for the exchange of phospholipids. Larger clusters containing several vesicles are formed where each vesicle can make multiple contacts if sterically allowed. In this paper we show that the overall process can be dissected into three functional steps: binding of PxB to vesicles, formation of stable vesicle−vesicle contacts, and exchange of phospholipids. Polycationic PxB binds to anionic vesicles. Formation of molecular contacts and exchange of monoanionic phospholipids through PxB contacts does not depend on the chain length of the phospholipid. Only monoanionic phospholipids (with methanol, serine, glycol, butanol, or phosphatidylglycerol as the second phosphodiester substituent in the head group) exchange through these contacts, whereas dianionic phosphatidic acid does not. Selectivity for the exchange was also determined with covesicles of phosphatidylmethanol and other phospholipids. PxB does not bind to vesicles of zwitterionic phosphatidylcholine, and its exchange in covesicles is not mediated by PxB. Vesicles of dianionic phospholipids, like phosphatidic acid, bind PxB; however, this phospholipid does not exchange. The structural features of the contacts are characterized by the spectroscopic and chemical properties of PxB at the interface. PxB in intermembrane contacts is readily accessible from the aqueous phase to quenchers and reagents that modify amino groups. Results show that PxB at the interface can exist in two forms depending on the lipid/PxB ratio. Additional studies show that stable PxB-mediated vesicle−vesicle contacts may be structurally and functionally distinct from "stalks", the putative transient intermediate for membrane fusion. The phenomenon of selective exchange of phospholipids through peptide-mediated contacts could serve as a prototype for intermembrane targeting and sorting of phospholipids during their biosynthesis and trafficking in different compartments of a cell. The protocols and results described here also extend the syllogistic foundations of interfacial equilibria and catalysis.

Polymyxin B (PxB)[1] is a cyclic amphipathic decapeptide with five positively charged side chains and an acyl chain at the N-terminus (Storm et al., 1977):

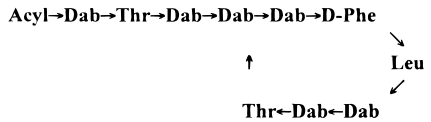

(Dab = α,γ-diamino-L-butyric acid)

We have shown that PxB mediates direct intervesicle exchange of DMPM by establishing stable intermembrane molecular contacts between vesicles without vesicle fusion or solubilization (Jain et al., 1991; Cajal et al., 1995, 1996). The PxB-mediated exchange of phospholipids occurs without net transfer, because integrity of vesicles in contact is maintained. This is expected in a contact between identical vesicles: even though the surface energy of small vesicles is not favorable, mixing of inner monolayers is not mediated by PxB.

Operationally, it is possible to dissociate at least three steps that lead to the formation of a functional contact between two vesicles: binding of PxB to the surface, apposition of two bilayers to form a stable vesicle−vesicle contact, and selective exchange of phospholipids through the contact. In this paper we describe criteria and protocols to dissect these steps and show that PxB promotes exchange of monoanionic

† This work was supported by Grant GM29703 from National Institutes of Health. Y.C. was supported by a postdoctoral fellowship from the Ministry of Science and Education (Spain).

* To whom correspondence should be addressed.

‡ University of Delaware.

§ Permanent address: Molecular Biophysics Unit, Indian Institute of Science, Bangalore, India.

⊗ Abstract published in *Advance ACS Abstracts,* April 15, 1996.

[1] Abbreviations: CL, Tetralauroylcardiolipin; Dab, α,γ-diaminobutyric acid; DMPX, 1,2-dimyristoylglycero-*sn*-3-phosphatidic acid (DMPA), or the corresponding phosphodiester with -choline (DMPC), -butanol (DMPBut), -glycerol (DMPG), -glycol (DMPGly), -methanol (DMPM), -serine (DMPS); DPPM, 1,2-dipalmitoylglycero-*sn*-3-phosphomethanol; DSPM, 1,2-distearoylglycero-*sn*-3-phosphomethanol; DTPA, 1,2-ditetradecylglycero-*sn*-3-phosphate; DTPM, 1,2-ditetradecylglycero-*sn*-3-phosphomethanol; E*, enzyme bound to the interface; K_{SV}, Stern−Volmer quenching constant; LPA, lysophosphatidic acid; LPC, lysophosphatidylcholine; LPM, lysophosphatidylmethanol; NBD-PE, *N*-(7-nitro-2,1,3-benzoxadiazol-4-yl)dioleoylphosphatidylethanolamine; PLA2, phospholipase A_2 from pig pancreas; PxB, polymyxin B; PxE, polymyxin E or colistin sulfate; PyPX, 1-hexadecanoyl-2-(1-pyrenedecanoyl)glycero-*sn*-3-phosphate (PyPA) and the corresponding-*sn*-3-phosphodiesters (PyPM or PyPC); Rh-PE, N-(lissamine rhodamine B sulfonyl)dioleoylphosphatidylethanolamine; TNBS, 2,4,6-trinitrobenzenesulfonic acid.

S0006-2960(95)02703-6 CCC: $12.00

phospholipids such as DMPM but not of dianionic phosphatidic acid, although vesicle−vesicle contacts are formed in both cases. Results with covesicles containing DMPM show that DMPA or DMPC do not exchange across PxB-mediated contacts between covesicles, although DMPM does. Structural and organizational constraints of PxB-mediated contacts are explored by chemical and spectroscopic methods. There are differences in the spectroscopic properties and chemical reactivity of PxB bound to DMPM or DMPA vesicles. Results also show that PxB in contacts is readily accessible from the aqueous phase and that the chemical reactivity and spectroscopic properties of PxB in the interface are different compared to those of PxB in the aqueous phase. Spectroscopic signatures of two forms of PxB at the interface can be dissected which suggests that the properties of PxB in the vesicle−vesicle contacts are different compared to those of PxB bound to the interface but not in an intervesicle contact. These differences are emphasized by the models compared in Figure 12. Broader significance of intermembrane interactions is discussed in the context of phospholipid transfer through peptide mediated contacts. It may also be emphasized for the benefit on the uninitiated reader that, in such a system, valid inference can be drawn only from a syllogistic interpretation of the sequence of addition. This is necessitated by the fact that the local and global conditions in a microscopically heterogeneous system can be very different, and the valid inference can only be drawn from the microscopic relations.

EXPERIMENTAL PROCEDURES

Materials. Pyrene-labeled phospholipids (with PC, PM, and PA head group) were purchased from Molecular Probes. DMPA (monosodium salt), DMPS (sodium salt), DMPG (sodium salt), DMPC, and the NBD- and Rhodamine-phospholipids labeled at the amino group of phosphatidylethanolamines were from Avanti. CL was kindly provided by Dr. J. Marecek (Stony Brook). LPC was from Calbiochem. Polymyxin B sulfate (PxB) and colistin methanesulfonate were from Sigma, and polymyxin E sulfate (PxE or colistin sulfate) was from Waco Ltd. (Japan). The purity and identity of these peptides was confirmed by analytical HPLC, amino acid analysis, and fast atom bombardment mass spectrometry (FAB-MS). Preparation of PLA2 from pig pancreas and all other phospholipids and lysophospholipids (lithium or sodium salts) used in this study have been described before (Jain et al., 1986a).

Vesicle Preparation. All spectroscopic and kinetic studies reported in this paper were carried out on small unilamellar vesicles obtained by sonication of the phospholipid powder dispersed in water above their gel−fluid transition temperature. Co-vesicles of DMPM containing other phospholipids or vesicles containing fluorescent probes were prepared by evaporation of a mixture of the lipid solutions in $CHCl_3$/CH_3OH (3:2). The dried film was hydrated and then sonicated (Lab Supplies, Hickesville, NY, Model G112SPIT) until a clear dispersion was obtained (typically 2−4 min).

Kinetic Measurements. Experimental protocols and conditions are adopted from those described elsewhere (Cajal et al., 1996). Protocols for monitoring the time course of hydrolysis of vesicles in the highly processive scooting mode (Jain et al., 1986, 1995; Berg et al., 1991) and for the interpretation of the reaction progress in the presence of PxB (Jain et al., 1991; Cajal et al., 1996) have been described in detail. Specific experimental conditions are given in the text or the figure captions; however, general protocols may be noted. Progress curves for the hydrolysis of phospholipid vesicles were obtained on a (Radiometer) pH-stat titration assembly where the stirrer speed is about 2000 rpm. Protocols for obtaining the size of vesicles and the amount of substrate available in the reaction mixture for the hydrolysis by PLA2 are as before (Cajal et al., 1995). Based on the total substrate present in the reaction mixture, it was found that typically about 65% of the total substrate was accessible to the enzyme added to the reaction mixture.

Precautions for handling PxB and for monitoring its effects on the reaction progress on DMPM vesicles are described in detail for DMPM (Cajal et al., 1996). The same precautions are necessary with other anionic phospholipids because the enzyme and PxB bind rapidly and do not exchange between vesicles. Vesicle−vesicle contacts mediated by PxB are stable for at least several minutes such that PxB or vesicles in contact do not exchange. The substrate and the products of hydrolysis do not exchange between vesicles except through the PxB contacts whose specificity is investigated in this paper. All studies reported here were carried out at low mole fractions of PxB where there is no indication of fusion or solubilization of vesicles induced by PxB. To avoid complications due to fusion during the reaction progress by PLA2 on DMPA (co-)vesicles, it was necessary to keep the calcium concentration below 0.1 mM; in all other cases calcium concentration could be kept at 0.5 mM without any detectable fusion for at least 30 min. It may be noted that calcium is not required for the PxB-mediated vesicle−vesicle exchange of phospholipids nor does it mediate exchange of phospholipids at the concentrations used for the kinetic studies (Cajal et al., 1996): the apparent dissociation constant for calcium for the catalytic turnover of PLA2 on DMPM vesicles is about 0.09 mM (Yu et al., 1993).

Fluorescence Measurements. Spectroscopic measurements were carried out at 25 °C in 10 mM Tris at pH 8.0 on an AB-2 spectrofluorimeter (SLM-Aminco) with constant stirring. All spectral manipulations were also carried out with the software provided with the instrument. Typically, the slit widths were kept at 4 nm each, and the sensitivity (PMT voltage) was adjusted to 1% for the Raman peak corresponding to the same excitation wavelength from the buffer blank. The relative change in the fluorescence, δF, is defined as: $(F - F_o)/F_o$, where F_o and F are the intensity without and in the presence of PxB, respectively. The exchange of lipid between vesicles on the addition of PxB was assessed by monitoring transfer of pyrene-labeled phospholipids as donor vesicles to an 100-fold excess of unlabelled phospholipid vesicles as acceptors. Fluorescence emission was monitored at 395 nm (with excitation at 346 nm) corresponding to the monomer emission.

Vesicle preparations used for the resonance energy transfer measurements contained 0.6% of NBD-PE or Rh-PE codispersed with suitable unlabeled lipids. Excitation was at 460 nm, and fluorescence emission from rhodamine was monitored at 592 nm. The change in fluorescence was calculated as $[F - F_o]/[F_\infty - F_o]$, with F_o and F corresponding to the fluorescence intensities before and after adding PxB, and F_∞ as the fluorescence after total mixing of lipids, as measured with co-vesicles containing 0.3 mol % of each of the probes at the same total bulk lipid concentration. This protocol was

also used to monitor (hemi)fusion-induced dilution of the probes in excess unlabeled vesicles.

Quenching Experiments. Changes in phenylalanine fluorescence spectra of PxB were recorded at the excitation wavelength of 256 nm using 4 nm bandwidths, in 10 mM Tris at pH 8.0 and 25 °C with constant stirring. Appropriate amounts of lipid vesicles were added to a solution of 50 μM PxB in the cuvette; spectra were recorded after equilibration (about 30 s). To monitor quenching of phenylalanine fluorescence signal by iodide or acrylamide, the quencher was added in increasing amounts from a stock solution in water: 1 M KI containing 0.25 mM $Na_2S_2O_3$ (to prevent I_2 and I_3^- formation) or 3.3 M acrylamide. Since the fluorescence emission intensity from phenylalanine is quite low, several corrections were necessary after subtracting the dark current of the instrument. The emission maximum was at 282 nm after correction for the light scattering and Raman peak of the buffer. These corrections were made by subtracting the spectra obtained under identical conditions using the non-fluorescent analogue PxE (Leu[6] instead of Phe[6]), which shows the same phospholipid exchange behavior as PxB. The fluorescence intensity readings were also corrected for the inner filter effect due to quencher absorption, according to $F = F_m f_Q$, where F is the corrected fluorescence intensity, F_m is the measured intensity after correction for scattering, and f_Q is the correction factor determined in a parallel titration with PxE, defined as the ratio of the signal in the absence of quencher with the signal obtained at a specified quencher concentration. Quenching results were analyzed according to Stern−Volmer equation for collisional quenching: $F_o/F = 1 + K_{SV}[Q]$, where F_o and F are the fluorescence intensities in the absence and presence of quencher, [Q] is the molar concentration of quencher, and K_{SV} is the Stern−Volmer quenching constant. Values of the Stern−Volmer constant for free phenylalanine or for PxB were of the same magnitude. Since the fluorescence life-time for phenylalanine is about 5 ns (Lorey et al., 1971), the quenching constant is in the range of 10^{10} M^{-1} s^{-1} which suggests that the quenching mechanism is collisional.

Light Scattering. The change in turbidity was measured as the change in the 90° scattered intensity at 360 nm and 1 nm slit widths on a SLM-Aminco AB-2 spectrofluorimeter. The relative change in the intensity of the scattered light, δI, is defined as for the fluorescence intensity.

Circular Dichroism Measurements. The CD spectra were typically recorded on a Jasco J700 spectropolarimeter in 1 or 10 mm cells with 1 nm slit width, at 25 °C in 10 mM Tris at pH 8.0. Five scans were recorded and averaged to improve the signal to noise ratio. The spectrum of buffer or blank vesicles was subtracted from the CD spectrum of the sample. For calculations of molar ellipticities, the concentration of the peptide was calculated by amino acid analysis of the acid hydrolysate on a Beckman System 6300 Autoanalyzer. Special care was taken to avoid possible artifacts due to light scattering from the vesicles in the presence of PxB. There is no noticeable path length dependence (the same CD signal is obtained in cells of 10 and 1 mm, with the exception that with 10 mm cell it is not possible to scan below 190 nm). Also in experiments with PxB in the presence of sodium dodecyl sulfate, essentially the same CD signal was obtained as in the presence of DMPM vesicles.

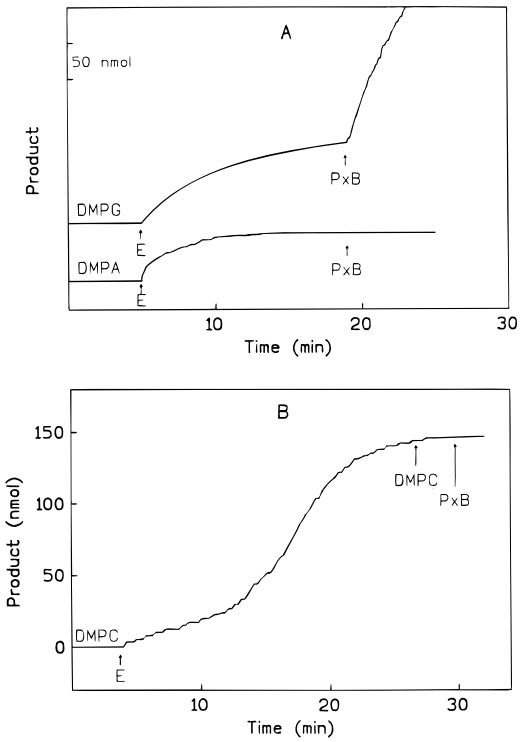

FIGURE 1: (A) Reaction progress curves for the hydrolysis of small sonicated vesicles of (top) DMPG (1 μmol in 4 mL of 0.5 mM $CaCl_2$ and 1 mM NaCl at pH 8.0) and (bottom) DMPA (1.1 μmol in 4 mL of 0.1 mM $CaCl_2$ and 100 mM NaCl at pH 8.0). The reaction was initiated with (20 pmol) PLA2 from pig pancreas, and after cessation of the catalysis PxB (11 nmol) was added to the reaction mixture. (B) Reaction progress curve for the hydrolysis of vesicles of DMPC (295 nmol) by PLA2 (26.5 pmol) in 4 mL of 0.5 mM $CaCl_2$ and 1 mM NaCl at pH 8.0. At the end of the hydrolysis, a fresh aliquot of DMPC (295 nmol) was added, followed by PxB (55 nmol).

Determination of the Number of Amino Groups Modified with TNBS. Reactivity of the five γ-amino groups of Dab residues in PxB (cationic at physiological pH) to TNBS was determined according to Fields (1972) on a UV spectrophotometer (Hewlett-Packard, Model 8452A). In short, the reaction in the cuvette was initiated by adding excess TNBS (10 mM) to a solution of 10 μM PxB in 0.025 M borate buffer at pH 9.5 containing 1 mM Na_2SO_3 with appropriate amount of lipid vesicles, if present. The solution was rapidly mixed (<10 s), and the formation of the TNB-amino group complexes was monitored by continuously recording the UV absorption at 420 nm. Each reaction progress curve was corrected for the time-dependent change in the reagent by subtracting the corresponding curve obtained under identical conditions but in the absence of peptide. Modification per amino group was calibrated with 1,8-diaminooctane, with the experimentally measured extinction coefficient of 19 000 M^{-1} cm^{-1} per amino group. This value is in accord with the reported values (Fields, 1972). Experimental curves were analyzed by least square nonlinear regression fitting to one or more exponential processes (GraphPad Inplot, San Diego, CA).

RESULTS

Effect of the Phospholipid Structure on the PxB-Mediated Exchange. The effect of PxB on the hydrolysis of vesicles of DMPG or DMPA by PLA2 is shown in Figure 1A. In both cases hydrolysis starts immediately after the addition of the enzyme. With less than one enzyme per six vesicles,

the reaction progresses until a constant number of phospholipids per enzyme are hydrolyzed; excess substrate vesicles present in the reaction mixture are not accessible to the bound enzyme. According to Poisson distribution, under these conditions each enzyme containing vesicle has at most one enzyme molecule; therefore, the extent of hydrolysis per enzyme is the number of accessible substrate molecules (= N_S), which also corresponds to the number of phospholipids present in the outer monolayer of a vesicle (Berg et al., 1991). As discussed in detail elsewhere for DMPM vesicles, this behavior is characteristic for the hydrolysis of vesicles in the scooting mode where the enzyme bound to vesicles does not exchange with excess vesicles, nor do the substrate or products of hydrolysis (Jain et al., 1995). Based on such criteria, hydrolysis of DMPG and DMPA vesicles, as well as that of DMPS and DMPGly (results not shown), occurs in the highly processive scooting mode.

As shown in Figure 1A, at the end of the reaction progress for DMPG vesicles, hydrolysis of excess vesicles is reinitiated immediately after the addition of PxB. The extent of hydrolysis in the second phase depends on the amount of PxB added, and at about 40 PxB molecules per vesicle virtually all the substrate present in the outer monolayer of DMPG vesicles (about 65% of the total) is hydrolyzed. This effect of PxB on the reaction progress for the hydrolysis of DMPG is similar to that reported for DMPM vesicles (Cajal et al., 1996). Essentially the same effect of PxB was observed with DMPS, DMPGly, and DMPBut vesicles (results not shown). In analogy with the results with DMPM, such observations show that PxB promotes vesicle−vesicle exchange of these monoanionic phospholipids, i.e., at least qualitatively, PxB promoted exchange has little head group specificity for monoanionic phospholipids. Since the initial rate of hydrolysis with the large vesicles in the absence of PxB is the same as that in the presence of PxB, these results also show that for phospholipids with different head groups the rate of exchange mediated by PxB is significantly faster than the rate of their hydrolysis ($\approx$300 s^{-1}) which, at least in the case of DMPM vesicles, is limited by the chemical step of the catalytic turnover cycle (Jain et al., 1992).

PxB mediates the exchange of monoanionic phospholipids of different fatty acid composition. The rate of hydrolysis is inversely proportional to the length of the fatty acids (DMPM > DPPM > DSPM), and the chemical step of the catalytic cycle remains rate limiting. PxB has no effect on the hydrolysis of DMPA and DMPC vesicles. The basis for the effect of PxB on DMPA or DMPC vesicles is appreciably different, although in both cases the intervesicle exchange is not promoted. For example, as shown in Figure 1A, PxB added at the end of the reaction progress for the hydrolysis of DMPA vesicles does not initiate the hydrolysis of excess vesicles. By the same criterion, the acidic phospholipid cardiolipin (diphosphatidylglycerol) is transferred through PxB-mediated vesicle−vesicle contacts (results not shown). Although each molecule of CL has effectively two negative charges, the charges are apparently sufficiently farther apart so as to be recognized as a pair of molecules of monoanionic phospholipids by PxB rather than as a dianionic phosphate like DMPA.

As shown in Figure 1B, hydrolysis of DMPC vesicles follows a complex course of reaction progress (Upreti & Jain, 1980; Apitz et al., 1982; Jain et al., 1989; Jain & Berg, 1989). Initially, the affinity of PLA2 for DMPC vesicles is poor, and the rate of hydrolysis is low during the latency period;

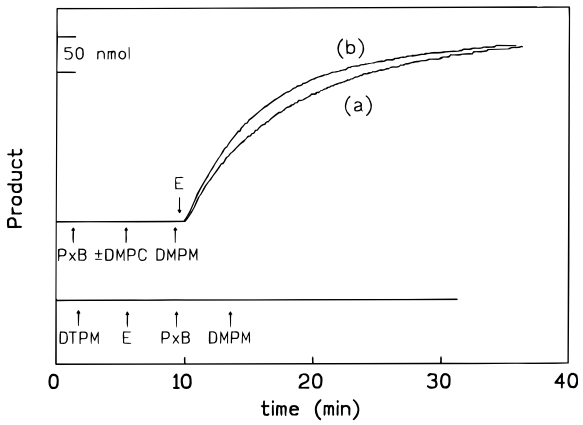

FIGURE 2: Effect of PxB on the reaction progress curves for the hydrolysis of DMPM and DMPC vesicles under different sequences of addition of the essential components. (Top) Reaction progress curve for the hydrolysis of DMPM (952 nmol) vesicles in 4 mL of 0.5 mM $CaCl_2$, 1 mM NaCl, and PxB (1.37 nmol) in the presence (a) or absence (b) of DMPC (295 nmol) vesicles. Reaction was initiated by PLA2 (5 pmol). (Bottom) DTPM (300 nmol) + E (36 pmol) + PxB (3 nmol) + DMPM (1.3 μmol).

as the products of hydrolysis accumulate more enzyme binds and virtually all accessible DMPC is hydrolyzed. As shown in Figure 1B, DMPC vesicles added at the end of the reaction progress are not hydrolyzed even after the addition of PxB, which suggests that the substrate replenishment for the PLA2 bound to vesicles of the products of DMPC is not promoted by PxB.

Possible origin of the inability of PxB to promote intervesicle exchange on DMPA or DMPC was investigated in detail by experiments designed on the basis of the following rationale. The effect of PxB on the exchange of DMPM (Cajal et al., 1996) showed that the transfer of phospholipids occurs through molecular contacts formed by PxB between the vesicles. This requires that PxB must bind to vesicles, that bound PxB forms the vesicle−vesicle contact, and that the exchange occurs through such contacts. A defect in any of these three steps would result in the loss of phospholipid exchange as monitored by the substrate replenishment assay (cf. Figure 1).

As elaborated below by kinetic and spectroscopic methods, it is possible to discern the origin of the differences in the effects of PxB described above. It may be remarked that, for the interpretation of the kinetic results, the order of addition of components is critically important for a proper distribution of the components on vesicles; random mixing of the components in the reaction mixture would lead to entirely different results. In fact, a strict sequence of addition of the components to a vigorously stirred reaction mixture forms a basis for several experiments described in this paper. Virtually a syllogistic interpretation of the sequence of addition of components is necessary to arrive at a specific inference about the properties of the vesicle−vesicle exchange of phospholipids mediated by PxB. This is a necessary consequence of the fact that, in a microscopically heterogeneous system, the local and global conditions can be very different, and the valid inference can only be derived from the microscopic relations.

PxB Does Not Bind to DMPC Vesicles. Binding of PxB to DMPC vesicles could not be demonstrated under a wide range of conditions. For example, as shown in Figure 2 (top), the progress curve for the hydrolysis of DMPM vesicles (present as clusters in the presence of PxB) is not

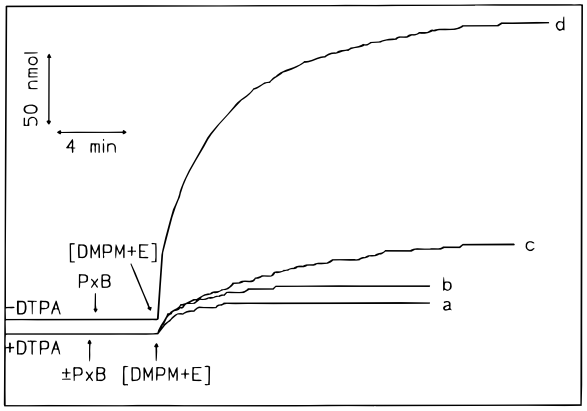

FIGURE 3: Effect of PxB on the hydrolysis of DMPM vesicles in the presence of DTPA vesicles. DTPA (340 nmol) + PxB (0, 0.825, and 1.65 nmol, curves a, b, and c, respectively). Control: curve d is as in c but no DTPA was added.

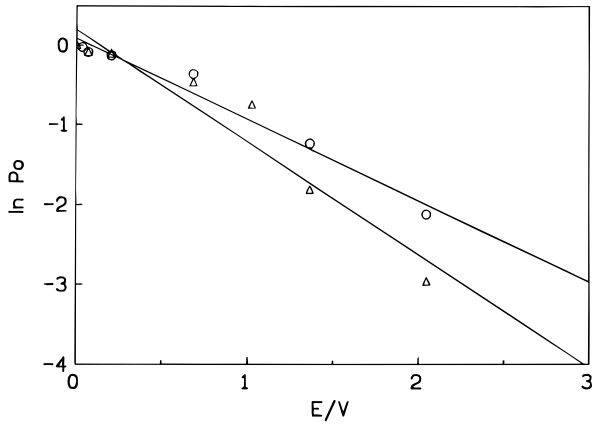

FIGURE 4: Poisson plot of ln P_o versus enzyme/vesicle ratio for DMPA vesicles in the (○) absence, slope 1.007 ± 0.073, or (△) presence of 30 PxB/vesicle, slope 1.415 ± 0.168. P_o is defined as the fraction of the total hydrolyzable substrate that is not hydrolyzed.

altered in the presence of DMPC vesicles. In this sequence of addition, DMPC vesicles have no effect because all the enzyme and PxB is taken up by DMPM vesicles. If PxB could bind to DMPC vesicles, it would not be available for the binding to DMPM vesicles added afterwards. On the other hand, PxB and PLA2 bound to DTPM vesicles are not available for the hydrolysis of DMPM vesicles (Figure 2, bottom). Under these conditions, if PxB was not bound to DTPM, or if it could exchange between vesicles, it would establish contacts between DMPM and DTPM vesicles, and resulting exchange would initiate hydrolysis of DMPM. For additional controls, see Cajal et al. (1996). Results in Figures 1B and 2 show that PxB does not promote transfer of DMPC to DMPC vesicles and that PxB added to DMPC vesicles is readily accessible to DMPM vesicles added subsequently. Other relevant controls for these experiments come from the spectroscopic studies described later; however, results described so far collectively show that cationic PxB does not bind to zwitterionic DMPC vesicles, thus implying that hydrophobic interactions are not critical as such. This is an expected result, and it is also supported by independent evidence (Zidovetzki et al., 1988; Sixl & Watts, 1985). In this context, it should be noted that colistin methanesulfonate derivative does not support exchange of anionic or zwitterionic phospholipids; it has only three positively charged γ-amino groups of Dab.

PxB Binds to DMPA Vesicles. As shown in Figure 1A, hydrolysis of DMPA vesicles occurs in the processive scooting mode; however, PxB does not promote transfer of excess DMPA to the enzyme-containing vesicles. This effect is not due to a lack of binding of PxB to DMPA vesicles. As shown in Figure 3, the extent of hydrolysis of a mixture of DMPM vesicles and PLA2 added to PxB is largely due to formation of clusters (compare sequence d with a). The extent of hydrolysis is relatively modest when the mixture is added to DTPA in the absence of PxB (sequence a) or in the presence of PxB (sequences b and c). Control experiments (not shown but carried out under the conditions of sequence d) also showed that DTPA vesicles added during the reaction progress had no effect on the time course, which suggested that DTPA is not spontaneously accessible to the enzyme-containing DMPM cluster. These results indicate that PxB effectively binds to DTPA vesicles and that most of the bound PxB is not available for making contacts between DMPM vesicles where hydrolysis occurs. Based on these results alone, it is not possible to discern whether or not PxB bound to DTPA forms contacts with DMPM vesicles.

PxB Does Not Form Functional Contacts between DMPA Vesicles. The effect of PxB on the Poisson distribution of PLA2 on DMPA vesicles is shown in Figure 4. Both in the absence and in the presence of 30 PxB/vesicle, a slope of 1 and 1.4, respectively, is obtained, which shows that in both cases the random Poisson distribution of PLA2 leads to the hydrolysis of one vesicle per enzyme (Berg et al., 1991). The slope of 1 in the absence of PxB indicates that the mechanism of action or the state of aggregation of the enzyme on DMPA interface is not noticeably different than that seen with DMPM vesicles (Cajal et al., 1995, 1996). In contrast to results with DMPM vesicles, the fact that the slope of the Poisson plots does not change significantly in the presence of PxB indicates that functional contacts between DMPA vesicles leading to substrate replenishment are not formed.

DMPC or DMPA Do Not Exchange through Functional PxB Contacts between Co-Vesicles Containing DMPM. Since PxB mediates contacts between vesicles of DMPM or its products of hydrolysis by PLA2, the ability of such contacts to mediate exchange of other phospholipids present in co-vesicles containing the contact-forming DMPM was examined. For example, as shown in Figure 5, co-vesicles of DMPA containing 12 mol % DMPM form functional contacts with other co-vesicles or with DMPM vesicles. Sequence A shows that all the available substrate in co-vesicles (both DMPA and DMPM) is hydrolyzed by the excess enzyme added initially. At the end of the reaction progress, all the enzyme is bound and it is not available for the hydrolysis of DMPM vesicles added afterward; however, with PxB added last, DMPM from the excess vesicles is transferred across the PxB contact formed with the PLA2-containing co-vesicles, where both DMPM and DMPA have been hydrolyzed.

Sequence B in Figure 5 shows that only DMPM is transferred across PxB contacts between co-vesicles of 12% DMPM in DMPA. PLA2 added to excess co-vesicles hydrolyzes only a small fraction of vesicles, as expected on the basis of Poisson distribution of enzyme over vesicles. However, PxB added after the cessation of hydrolysis causes additional hydrolysis which corresponds to the amount of DMPM present in the outer layer of the excess vesicles (curve a). As shown by curve b, the same amount of PxB

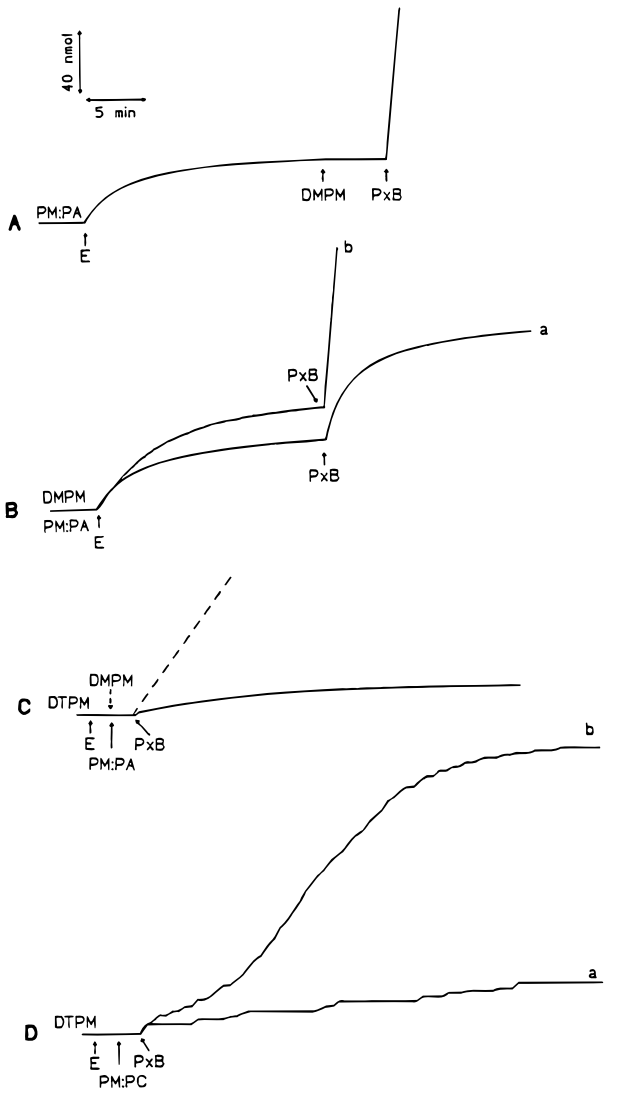

FIGURE 5: PxB-mediated lipid transfer between co-vesicles monitored by the reaction progress curves of hydrolysis under different sequences of addition. (A) DMPM/DMPA co-vesicles (60 nmol) were hydrolyzed with excess PLA2 (40 pmol), and then DMPM vesicles (952 nmol) and PxB (22 nmol) were added sequentially. (B) Curve a, hydrolysis of DMPM/DMPA co-vesicles (976 nmol) was initiated by PLA2 (19.8 pmol), and after cessation of the hydrolysis PxB (11 nmol) was added to the reaction mixture; curve b, similar conditions as above but with DMPM (952 nmol) vesicles. (C) PLA2 (238 pmol) was added to DTPM (498 nmol), and DMPM/DMPA co-vesicles (325 nmol) were added afterward, followed by PxB (9.3 nmol). As a control, it must be noted that addition of PxB to a mixture of DTPM containing enzyme and DMPM induces a fast substrate replenishment (dashed line). (D) To a mixture of DTPM (498 nmol) vesicles containing PLA2 (238 pmol) and DMPM/DMPC co-vesicles (298 nmol), PxB was added (0.582 and 1.45 nmol in curves a and b, respectively). PM = DMPM, PA = DMPA, and PC = DMPC.

added to DMPM vesicles allows hydrolysis of all the accessible substrate. These results show that DMPA present in excess co-vesicles is not transferred to the enzyme-containing co-vesicles. This interpretation is based on the assumption that vesicles of DMPM and DMPA behave the same as those of their products of hydrolysis. The fact that exchange of DMPM with DMPM or with products of its hydrolysis is indistinguishable has been shown independently (Jain et al., 1991; Cajal et al., 1996).

Selectivity for the exchange of DMPM, but not of DMPA, through PxB-mediated contacts is also supported by sequence C. PLA2 added to DTPM vesicles is not available for the

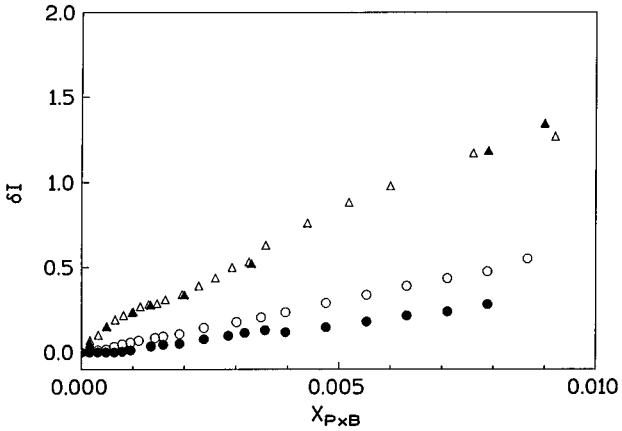

FIGURE 6: PxB induced changes in the intensity of 90° scattered light at 360 nm as a function of mole fraction of PxB for (△) DMPM (0.238 mM) in 10 mM Tris/1 mM EGTA, (▲) DMPM (0.238 mM) in 10 mM Tris/1 mM EGTA/26 mM NaCl, (○) DMPA (0.244 mM) in 10 mM Tris/1 mM EGTA, and (●) DMPA (0.244 mM) in 10 mM Tris/1 mM EGTA/26 mM NaCl.

hydrolysis of DMPM vesicles or of 12% DMPM in DMPA covesicles; however, in both cases the extent of hydrolysis after the addition of PxB corresponds only to the amount of DMPM present in the reaction mixture, that is, DMPA is not transferred to the enzyme containing vesicles.

Specificity for the exchange of DMPC across PxB-mediated vesicle−vesicle contacts formed between DTPM vesicles and co-vesicles of 12% DMPM in DMPC is shown by sequence D (Figure 5). PLA2 on DTPM vesicles is not available for the hydrolysis of the co-vesicles. If 0.1 mol % PxB (relative to DMPM) is added, hydrolysis is initiated immediately and only DMPM in co-vesicles is hydrolyzed (curve a). Surprisingly, however, at >0.3% PxB, DMPC is also hydrolyzed with a time delay. Such a behavior is expected if (hemi)fusion of vesicle has occurred under these conditions. In this paper we have not examined this possibility further. Control experiments showed that enzyme added directly to co-vesicles hydrolyzed both DMPM and DMPC [see also Ghomashchi et al. (1991)].

Spectroscopic Evidence for Apposition of Vesicles. Kinetic results summarized thus far are unique in the sense that they provide a rapid and continuous method for monitoring selective and direct vesicle−vesicle transfer of phospholipids that are substrates for PLA2. This method therefore provides a steady-state measure of the phospholipid substrate that the enzyme "sees" during the course of reaction progress. Independent spectroscopic protocols were developed that not only provide a measure of transfer of the probe phospholipid but also could dissect the steps for the formation of vesicle−vesicle contact and the transfer of phospholipids.

A change in the size of the particles is accompanied by a change in the turbidity. As shown in Figure 6, an increase in the 90° scattering of DMPM vesicles is observed in the presence of PxB. At any given mole fraction of PxB, the increase is significantly larger with DMPM vesicles than it is with DMPA vesicles. The increase with DMPA is somewhat lower in the presence of NaCl, whereas salt has no noticeable effect on the scattering change from DMPM vesicles.

Apposition of vesicles, whether or not they form functional contacts, was also monitored by resonance energy transfer (RET) that should occur if a vesicle containing the donor NBD probe comes within the energy transfer distance of a

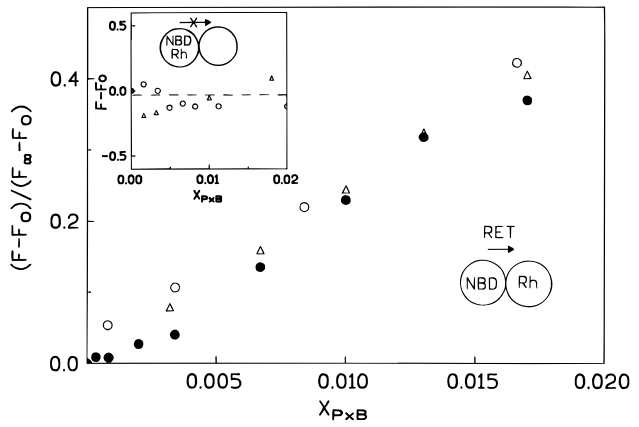

FIGURE 7: Increase in the resonance energy transfer (RET) intensity as a function of the mole fraction of PxB added to an equimolar mixture of vesicles containing 0.6% NBD-PE or Rh-PE in DMPM (○), DMPA (△), and DMPA with 26 mM NaCl (●). The total lipid concentration was 81.6 μM in Tris 10 mM. (Inset) Change in RET after mixing vesicles containing 0.3% of both probes (16.32 μM) with excess unlabeled vesicles (816 μM) in 10 mM Tris, upon addition of PxB: (○) DMPM, (△) DMPA.

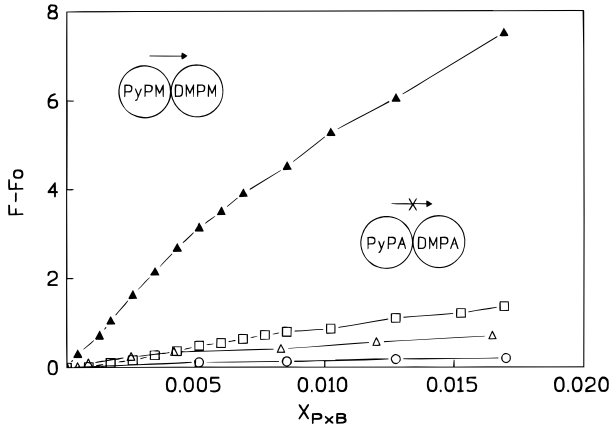

FIGURE 8: Fluorescence intensity of pyrene monomer as a function of PxB mole fraction in a mixture vesicles of PyPM with DMPM (▲), PyPA with DMPA (△), co-vesicles of 12% DMPM in PyPA with DMPM (□), and vesicles of PyPC with DMPC (○). Bulk lipid concentration was 1.25 μM for Py-vesicles and 159 μM for unlabeled acceptor vesicles, in 10 mM Tris, pH 8.0.

vesicle containing the acceptor Rh probe. Results in Figure 7 were obtained by mixing vesicles containing NBD-PE (0.6%) with vesicles containing Rh-PE (0.6%). The energy transfer distance of this pair is about 50 Å. No noticeable increase in the RET intensity at 592 nm (rhodamine emission) is seen on mixing of the vesicles. As shown in Figure 7, an increase in the energy transfer signal was observed in the presence of PxB, and a corresponding decrease (not shown) in the intensity was also observed at the emission from NBD (540 nm). The magnitude of the increase depends upon the mole fraction of PxB; however, essentially the same magnitude of energy transfer is induced by PxB whether the probes are codispersed in the DMPM or DMPA matrix. The fact that a comparable increase in the RET intensity is observed in the two pairs of matrices (PM-PM, PA-PA) suggests that close apposition of vesicles is induced by PxB between DMPM or DMPA vesicles. Formation of large clusters containing several vesicles at ~0.02 mole fraction PxB also accounts for a relatively large magnitude of the RET intensity (~40% compared to that seen with the total mixing of the probes). These results are entirely consistent with the kinetic results.

The possibility that the RET probes are mixed between vesicles in close apposition is eliminated by results shown in the inset to Figure 7, where ternary co-vesicles containing both the donor and acceptor probes (0.3% each) with a matrix lipid were mixed with an excess of DMPM or DMPA vesicles. In both cases, little change in the RET intensity at 592 nm was observed. A decrease is expected if the probes are diluted by lipid mixing (Struck et al., 1981), and such an effect was indeed seen at higher mole fraction of PxB where (hemi)fusion occurs.

Spectroscopic Evidence for Specificity for the Phospholipid Exchange. Having shown that PxB binds to DMPA vesicles, and that these vesicles are apposed in the presence of PxB, the spectroscopic evidence described next shows that functional vesicle−vesicle contacts are not formed between vesicles of phosphatidic acid. Transfer of phospholipids across PxB contacts was monitored as the change in the fluorescence intensity of pyrene-labeled phospholipids. Emission from vesicles of pyrene-phospholipid is dominated by the excimer band (480 nm), and the intensity of the monomer band (395 nm) increases as the probe is diluted due to its exchange with phospholipids from vesicles in contact. As shown in Figure 8, such an increase was observed on the addition of PxB to a mixture of vesicles containing PyPM with vesicles of DMPM, but not with pairs of vesicles of PyPA/DMPA, or PyPC/DMPC, or (PyPA+DMPM)/DMPM.

These results are entirely consistent with the conclusion that PxB-mediated functional vesicle−vesicle contacts are formed between DMPM and PyPM vesicles, whereas, in the case of DMPA, PxB induces close apposition between vesicles (Figure 7), but functional contacts leading to phospholipid exchange (Figure 8) are not formed. More striking is the observation that PyPA in co-vesicles with 12% DMPM does not transfer the PyPA probe to DMPM vesicles in the presence of PxB contacts. This is in agreement with the kinetic results with co-vesicles of DMPA and 12% DMPM shown in Figure 5.

The presence of two negative charges in the head group of DMPA, instead of only one in DMPM, apparently is not entirely responsible for the inability of DMPA to exchange through PxB-mediated contacts. The PxB-mediated lipid exchange between DMPM and 12% DMPM/PyPA vesicles was monitored at pH 5.2. Even under these conditions, where DMPA is monoanionic, there was no significant transfer of PyPA (data not shown). This suggests a more complex nature for the mechanism of selectivity in the functional PxB contacts, possibly due to a pK_a change in the phosphate head group complexed with PxB.

Collectively, these results clearly show that phospholipids with dianionic head group such as in DMPA or PyPA do not exchange through vesicle−vesicle contacts mediated by PxB. Also, DMPC and other lipids with probes (dansyl-, NBD-, or rhodamine-) in the head group region of the phospholipid do not cross the contact. On the other hand, probes (NBD, pyrene) attached to the acyl chain of monoanionic phospholipids are transferred (results for NBD are not shown).

Lysophospholipids Do Not Perturb the PxB-Mediated Exchange of Phospholipids. The possible effect of lysophospholipids in the PxB-mediated phospholipid exchange was evaluated by means of the fluorescence assay using a mixture of PyPM and DMPM vesicles. Exogenous lysophospholipids (LPC, LPM, or LPA) were added to DMPM

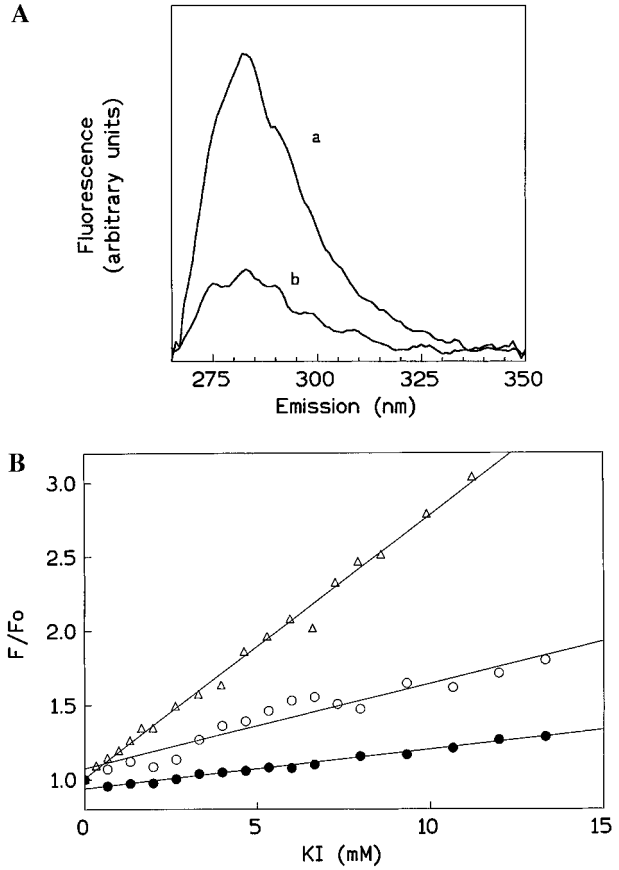

FIGURE 9: Quenching of PxB fluorescene. (A) Fluorescence emission spectra of PxB (50 μM) in the presence of DMPM vesicles (2.75 mM) before (a) and after (b) addition of KI (13.3 mM). Spectra are corrected for turbidity and Raman contribution of the buffer as described in Experimental Procedures. (B) Stern−Volmer plots showing the phenylalanine quenching of 50 μM PxB in buffer (△) and in the presence of DMPM vesicles at DMPM/PxB mole ratio 200:1 (○) and 60:1 (●), by the aqueous quencher I^-. Excitation was set at 256 nm, and emission was recorded at 282 nm; excitation and emission band passes were 4 nm.

vesicles 5 min before the addition of PyPM vesicles, so that the lysophospholipid is incorporated mainly in the outer monolayer of the DMPM vesicles (Jain et al., 1985). In other experiments, DMPM was sonicated in presence of the lysophospholipid to ensure its incorporation in both inner and outer monolayers. At 4.2 mol % lysophospholipid, the time course of the change in the pyrene fluorescence was recorded after the addition of PxB (0.43 mol %), with a time resolution of 0.5 s. No differences in the rate of fluorescence increase were observed with any of the lysophospholipids assayed; in all cases, the increase of fluorescence after PxB addition was virtually instantaneous and indistinguishable from the controls without additive. These results show that the lipids with propensity to change the surface curvature do not influence the kinetics of exchange and therefore the functional properties of the PxB-mediated intervesicle contacts.

Bound PxB Is Accessible from the Aqueous Phase. The fluorescence emission spectrum of PxB does not change significantly on binding to anionic vesicles. The degree of exposure of bound PxB was monitored as quenching of fluorescence emission from phenylalanine at 282 nm by two aqueous quenchers, iodide and acrylamide. An example of typical spectra of PxB bound to DMPM vesicles before and after addition of iodide is shown in Figure 9A. Stern−Volmer plots in Figure 9B show the effect of iodide on the

Table 1: K_{SV}, the Stern−Volmer Quenching Constants (M^{-1}) for the Quenching of Phenylalanine (50 μM) Fluorescence by Iodide and Acrylamide in Different Environments

conditions	KI[a]	acrylamide[a]
Phe (free)	63.3	43.8
PxB (free)	177.3	53.4
60:1 DMPM/PxB	26.2	87.5
200:1 DMPM/PxB	57.0	70.0
60:1 DMPA/PxB	46.5	47.6
200:1 DMPA/PxB	68.8	70.8

[a] All intensity values are corrected for turbidity and for inner filter effect before plotting (Figure 9B).

emission from PxB on DMPM vesicles. A key observation is that the fluorescence of PxB in buffer is readily quenched by iodide (K_{SV} is higher than that for free phenylalanine; see Table 1). This is expected because polycationic PxB would facilitate the binding of iodide. On the other hand, PxB bound to DMPM vesicles is 3−7-fold less accessible to iodide. There are two possible reasons for this difference: either the phenylalanine residue is shielded in the bound form of PxB or the negatively charged iodide is shielded from the bound PxB at the negatively charged surface of the vesicle. Results on quenching of phenylalanine by acrylamide support the second possibility. As summarized in Table 1, the Stern−Volmer constant for quenching by acrylamide does not change significantly on the binding of PxB to the interface. These results show that PxB bound to DMPM vesicles and in vesicle−vesicle contacts remains accessible from the aqueous phase; the possibility that the quencher promotes the removal of PxB from the vesicles was ruled out by kinetic protocols of the type shown in Figure 5. Thus it can be concluded that PxB in the contacts is not included inside a micellar or an hexagonal phase particle where it will become inaccessible from the bulk aqueous phase.

The magnitude of iodide quenching appears to depend on the lipid/peptide ratio (Figure 9B). At DMPM to PxB mole ratio of 200:1 (or at 30 PxB/V, where all PxB is in vesicle−vesicle contacts: PxB_c form), quenching is less efficient than that at 60:1 mole ratio (or at 100 PxB/V, where some PxB would be in contacts and the rest bound to the vesicle but not in contact: PxB_b form). This difference was not seen with acrylamide quenching. An interpretation that reconciles both results is that phenylalanine of PxB bound to DMPM vesicles remains completely accessible to aqueous phase (see acrylamide results), but PxB at the interface exists in two forms (PxB_c and PxB_b) neutralized by the anionic surface of the vesicles to a different extent. This will reflect in different iodide quenching efficiencies, simply because iodide is shielded from the peptide by the negatively charged phospholipid headgroups.

When the same experiment was carried out with DMPA vesicles (Table 1), essentially the same results were obtained: bound PxB remains accessible to acrylamide and iodide quenching, but in this case the Stern−Volmer constants for iodide seem to be independent of the lipid to PxB ratio, as if only one form of PxB exists in DMPA vesicles.

The Chemical Reactivity of PxB-Amino Groups is Different in DMPM or DMPA Vesicles. Additional information about the accessibility of PxB at the interface was obtained by monitoring the chemical reactivity of its free amino groups toward TNBS from the bulk aqueous phase. The progress

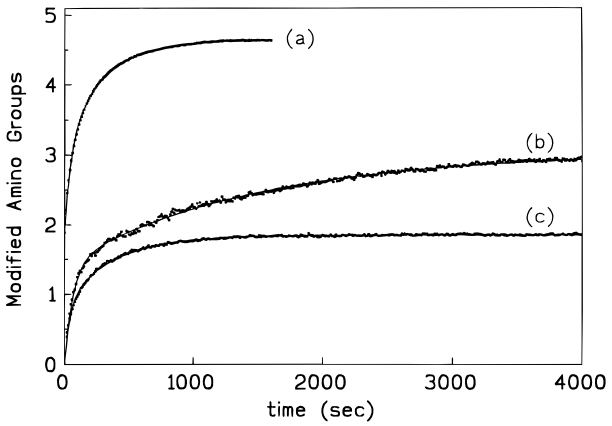

FIGURE 10: Reaction progress for the modification of PxB amino groups by TNBS: (a) PxB in buffer, (b) PxB with DMPA vesicles, (c) PxB with DMPM vesicles. Lipid concentration, 1.5 mM; PxB, 10 μM.

Table 2: Changes in the Extinction Coefficient (halftime for Modification in Seconds) at 420 nm on Incubation of PxB (10 μM) with TNBS (10 mM) at 25 °C

	A^a	B	C	no.[b]
PxB	37700 (<10s)	23 204 (32s)	31 942 (196s)	4.64
1:300 PxB/DMPM		16 896 (29 s)	20 186 (260 s)	1.85
1:150 PxB/DMPM		20 973 (49 s)	18 501 (294 s)	1.97
1:40 PxB/DMPM			39 393 (199 s)	1.96
1:300 PxB/DMPA		28 620 (47 s)	32 209 (1017 s)	3.04
1:150 PxB/DMPA		21 475 (56 s)	40 623 (1144 s)	3.1
1:40 PxB/DMPA			56 882 (806 s)	2.8

[a] *A*, *B*, and *C* are the extinction coefficients (M) for the three different species of amino groups in PxB with different reactivity to TNBS. [b] Number of amino groups that have reacted with TNBS.

curves for the modification of PxB under different conditions are shown in Figure 10. Such curves were analyzed by iterative least-squares fit to

$$y = A + B[1 - e^{-DX}] + C[1 - e^{-EX}]$$

Here *B* and *C* are the extinction coefficients corresponding to two different classes of amino groups with half times ($t_{1/2}$) 0.69/*D* and 0.69/*E*, respectively. The residuals were examined to ascertain goodness of fit and systematic departure. Fits were judged to be good within 1%. In the case of free PxB (Figure 10, curve a), the progress curve could be resolved into three components: the first component (species A), corresponds to the modification of about two amino groups (ϵ = 37 700 M^{-1} cm^{-1}) with $t_{1/2}$ of less than 10 s. The rest of the progress curve showed the presence of two other classes of modifiable amino groups: one (ϵ = 23 200 M^{-1} cm^{-1}) with a $t_{1/2}$ of less than 32 s (species B), and 1.6 amino groups (ϵ = 31 942 M^{-1} cm^{-1}) with $t_{1/2}$ = 195 s (species C). Such parameters obtained under a variety of conditions at different PxB/lipid ratios are summarized in Table 2, and the most significant conclusions are developed below.

TNBS does not penetrate lipid membranes; however, the reactivity of the amino groups to TNBS changes with the environment and accessibility. PxB bound to vesicles of DMPM does not show the fast-reacting amino groups with $t_{1/2}$ below 10s. seen with PxB in buffer, and only two of the five amino groups are derivatized (Figure 10, curve c). Under the conditions where all PxB is present in intervesicle contacts, i.e., the PxB_c form, (DMPM/PxB = 300:1 and 150:1, or 20 PxB/V, and 40 PxB/V, respectively), only two of the five amino groups are available to TNBS, with different reactivities: one (species B) around 30 or 50 s, and the other (species C) with $t_{1/2}$ around 280 s. Also under the conditions where excess PxB is present, and thus at least some PxB can be in the bound form but not involved in intervesicle contacts (PxB_b) as at DMPM/PxB 40:1, only two amino groups are derivatized with TNBS; apparently both are equally exposed, with $t_{(1/2)C}$ = 200 s.

When the same experiment was carried out with DMPA vesicles, where PxB cannot form functional intervesicle contacts for the transfer of phospholipids, the number of susceptible amino groups was three (Figure 10, curve b). The additional amino group that is not modified in PxB bound to DMPM belongs to the slow-reacting species C, with $t_{(1/2)C} \approx$ 1000 s (Table 2). These results clearly show that PxB in its two bound forms is accessible from the bulk aqueous phase; however, the chemical reactivities of the amino groups are appreciably altered.

Bound PxB Exists in Two Forms. CD spectra of 134 μM PxB in 10 mM Tris at pH 8 is shown in Figure 11A. It is dominated by a cross point at 188 nm, a strong band centered at 198 nm, and a shoulder at 217 nm. The magnitude of ellipticity and the presence of the shoulder indicate an ordered structure of PxB in aqueous solution, with a significant contribution of random coil or another rigid conformation (Shinnar et al., 1993). The same spectrum was obtained at pH 12, where all the amino groups are deprotonated. A significant induction of secondary structure in PxB is seen upon binding to negatively charged DMPM vesicles: the minima shifts to 203 nm, and the cross point to 194 nm. In addition, the magnitude of ellipticity of the spectra varies as a function of the lipid concentration, decreasing with increasing lipid ratio from 24:1 to 238:1 (Figure 11A). This decrease in spectral intensity upon dilution of the peptide at the bilayer surface is indicative of a conformational change affecting the peptide backbone. According to previous observations (Cajal et al., 1995, 1996), the ability of PxB to form intervesicle molecular contacts for the exchange of phospholipids (PxB_c) is maximum at around 30 PxB molecules per vesicle, which corresponds to a lipid/peptide mole ratio of 200:1. Accordingly, the CD spectra obtained at 238:1 mole ratio corresponds to the PxB_c species, whereas, with decreasing lipid ratio, the contribution from PxB bound to the interface (PxB_b), but not in contacts, increases. The difference spectrum corresponding to PxB_c (curve e-b in Figure 11B) was generated by subtracting the spectrum of PxB/DMPM at 1:24 mole ratio from the one in PxB/DMPM in 238:1 ratio. Similarly, a spectrum for the PxB_b form (b-a) was obtained by subtracting the spectrum of PxB in buffer from that in PxB/DMPM at 1:24 ratio.

Although we cannot yet assign a secondary structure responsible for the spectra shown in Figure 11, they certainly are not due to a random coil structure. The band corresponding to the PxB_c form (e-b) is reminiscent of a β-turn structure, with a maxima around 202 nm and a minima at 184 nm, whereas the band corresponding to PxB_b form (b-a) has a maximum at around 191 nm and a minima at 207 nm. No changes in the CD spectra are observed on the addition of PxB to DMPM vesicles at pH 12, thus indicating that the positive charges are necessary for the structural changes in PxB associated with its binding to anionic vesicles. It may also be noted that the CD signal of colistin methanesulfonate derivative corresponds to a random coil

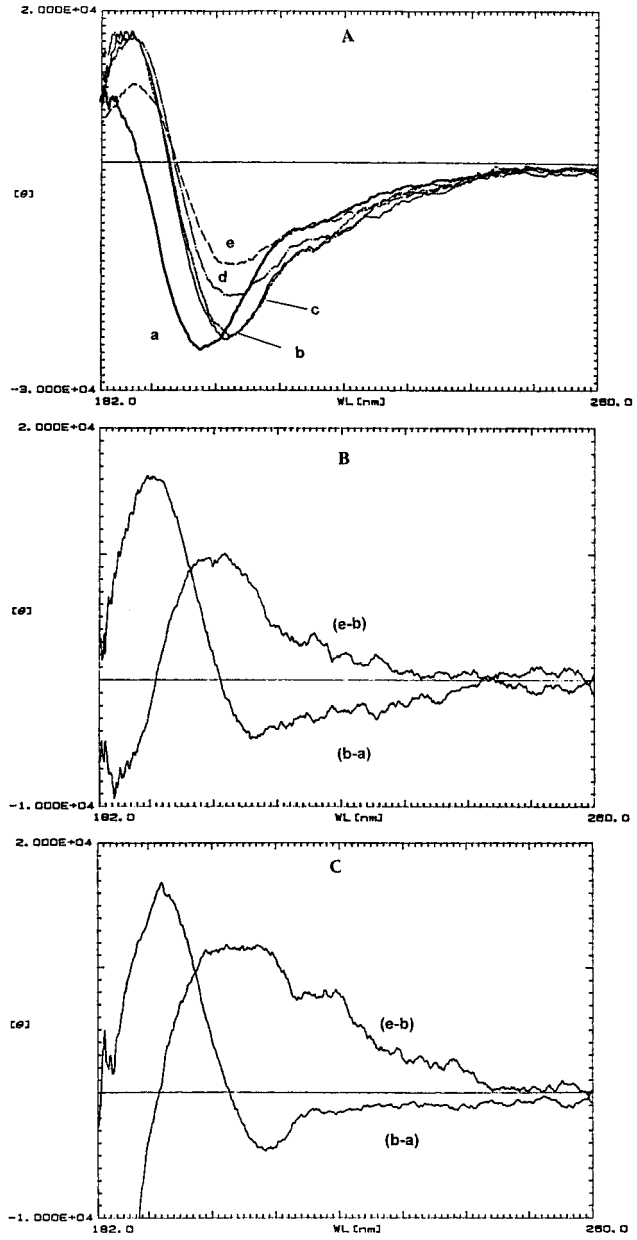

FIGURE 11: (A) Circular dichroism spectra of PxB (134 μM) in the presence of DMPM vesicles at lipid to PxB mole ratios: 0:1 (a), 24:1 (b), 60:1 (c), 119:1 (d), and 238:1 (e). (B) Difference spectra for PxB in DMPM at high lipid ratio (e-b) (PxB is in the contact form) and at low lipid ratio (b-a) (PxB is in the bound form, see text). (C) Difference spectra for PxB in DMPA at the same mole ratios as in panel B. Mean residue molar ellipticity [θ] is in deg cm^2 dmol^{-1}.

peptide in buffer, and no changes are observed in presence of DMPM.

The CD difference spectra resulting from the binding of PxB to DMPA vesicles are shown in Figure 11C. At low lipid to PxB ratios (e.g., 24:1), the difference spectrum (b-a) is comparable to those obtained in DMPM under comparable conditions. On the other hand, the difference spectra (e-b) corresponding to high lipid to PxB ratio (238:1) with these two lipids are noticeably different in shape and magnitude, indicating that PxB_c form in DMPM does not adopt the same structure in DMPA. As expected, no change in the secondary structure of PxB is induced by zwitterionic DMPC (result not shown). These results clearly show that the molecular conformation of PxB changes in different ways under different conditions at the interface.

Table 3: Specificity for the PxB-Mediated Exchange of Phospholipids: Three Sequential Steps That Lead to Formation of a Functional Intervesicle Contact Are Dissected

	PM/PM[d]	PA/PA	PM:PA/PM PM:PA/PM:PA	PC/PC	PM:PC/PM
binding[a]	+	+	+	−	+
apposition[b]	+	+	+	−	+
exchange[c]	+	−	+ PM − PA	−	+ PM − PC[e]

[a] Binding of PxB to the lipid vesible determined by kinetic and spectroscopic experiments. [b] Apposition between vesicles determined by 90° light scattering and RET. [c] Exchange of phospholipids between vesicles is measured by kinetics of hydrolysis by PLA2 and fluorescence spectroscopy (pyrene). [d] Results are extensible to different monoanionic phospholipids (DMPM, DPPM, DSPM, DMPG, DMPGly, DMPBut, DMPS). [e] PC can be transferred when PxB mole fraction is >0.3% (relative to DMPM).

DISCUSSION

Studies in this paper are designed to dissect three steps that lead to the formation of a functional intermembrane molecular contact mediated by PxB: binding of PxB, apposition of vesicles which may or may not involve formation of a functional contact between vesicles, and exchange of phospholipids through the molecular contact. As summarized in Table 3, results obtained with different protocols are useful in dissecting steps that lead to the formation of a functional contact. A striking conclusion of this study is that PxB contacts formed between co-vesicles containing the contact-forming DMPM with DMPA or DMPC permit exchange of DMPM but not of the other phospholipid. This raises interesting possibilities about the mechanistic significance and the structural basis for the selectivity. The reason for a lack of binding of polycationic PxB to zwitterionic interface is most probably the lack of the necessary electrostatic interaction. That PxB binds to, but cannot transfer, DMPA is particularly striking, because it implies that PxB bound to DMPA vesicles is in a different molecular state than that on vesicles of monoanionic phospholipids like DMPM, as supported by chemical and spectroscopic evidence. Besides extending the syllogistic foundations of interfacial catalysis and equilibria, the novel molecular phenomenon underlying the properties of PxB contacts has broad implications. As developed elsewhere (Cajal et al., 1995; Cajal & Jain, 1996), properties of PxB contacts provide a novel basis for its antibiotic activity by scrambling the phospholipid composition of the membranes surronding the periplasmic space in Gram-negative organisms. Such a mode of action is not expected to be overcome by stable genetic resistance. Two additional implications of the peptide-mediated contacts are discussed below.

Properties of PxB-Contact Are Different Than Those of "Stalk". Our working model for the structure of the PxB contact is shown in Figure 12, where its structural features are compared with those of a "stalk", the putative intermediate of membrane fusion (Chernomordik & Zimmerberg, 1995; Markin et al., 1984; Siegel, 1993). Despite obvious similarity in their structural conceptualization, functional differences may be emphasized. The model for contact is consistent with observations that the contacts are formed by a small number of PxB molecules, possibly six per contact (Cajal et al., 1996), that PxB in the contact remains exposed to the solvent (quenching and chemical modification experiments), and that the bilayer structure is maintained (kinetic and fluorescence results). The fact that the bilayer organiza-

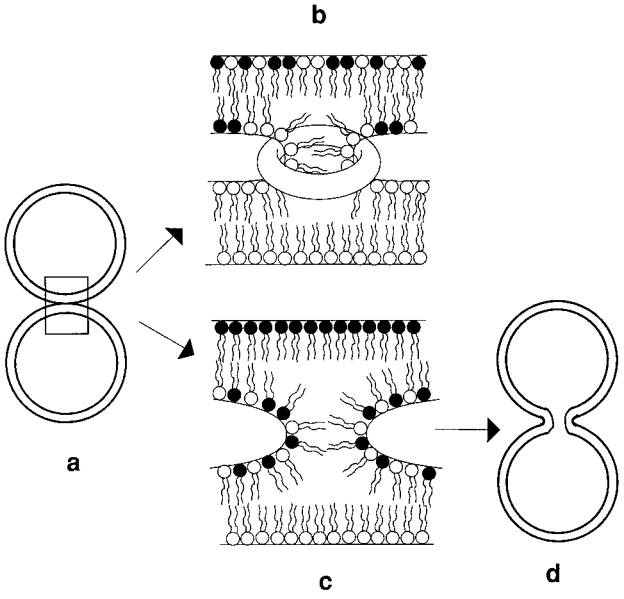

FIGURE 12: Schematic models for the hypothetical intermembrane interactions through PxB contacts or through "stalk". The cross-section of bilayers are shown with two different species of phospholipids to emphasize exchange through contacts and mixing through stalks. (a) Two membranes come in close apposition. (b) Working model for the molecular structure of PxB contacts where a complex formed by six PxB molecules brings together the outer monolayers of two vesicles, and phospholipids from the apposed monolayers selectively exchange through the opening in the middle of the contact. (c) Stalk, putatively the first intermediate for (hemi)fusion, brings in contact the two apposed monolayers. (d) A fusion pore formed from an expanded stalk as the probability of a chance contact between the inner monolayers increases.

tion is not altered by PxB suggests that all mechanisms invoking formation of soluble complexes of PxB with lipid may be eliminated from consideration. Similarly, all mechanisms based on fusion or hemifusion of vesicles are discounted because the intermembrane transfer of phospholipid through these contacts is selective, and lipid-mixing does not occur. Results reported here also show that the presence of additives (e.g., lysophospholipids) that prevent the formation of nonbilayer structures (Chernomordik et al., 1993; Vogel et al., 1993; Kozlov & Markin, 1983) do not play a role in the formation or function of the PxB contacts. The fact that PxB in the contacts is accessible to quenchers and chemical reagents from the aqueous phase also rules out the possibilities that invoke formation of intermembrane particles and related structures based on inverted micelles and hexagonal phase. This is because PxB sequestered in such particles would not be readily accessible from the bulk aqueous phase. These results along with the difference CD spectra (Figure 11) clearly show that specific molecular interactions of several PxB molecules with vesicles is most probably responsible for the formation of a complex that mediates selective exchange of phospholipids. Within constraints of these observations, an attractive possibility is that a torus of six PxB molecules forms the contact (Cajal et al., 1996). As implied in Figure 12, PxB is not a "catalyst" but an integral part of a stable functional contact. Such a role of PxB-mediated vesicle−vesicle contacts is dramatically different than that invoked in the properties of a transient "stalk" or TMC (transmonolayer contact), whose formation is driven by the curvature propensities of the component lipids. We are pursuing the mechanistic basis of such possibilities.

The heuristic and multistep character of the process of fusion between two membranes is emphasized by the various models that are being actively debated (White, 1992; Siegel, 1993; Schweizer et al., 1995; Vogel et al., 1993). The steps that have been described by consensus are the apposition or docking of membranes and the final fused membrane. Sincethe intermediates of fusion are believed to be of a highly transient nature, there is little experimental data on the molecular organization of the structures involved. Nevertheless, two types of intermediates have been proposed in the literature: the inverted micellar intermediate (Siegel, 1984, 1986a,b; Verkleij et al., 1979) and the stalk fusion intermediate (Chernomordik & Zimmerberg, 1995; Markin et al., 1984; Siegel, 1993). The inverted micellar intermediate cannot account for the observed fusion behavior of most lipid systems, whereas there is a great deal of data that favors the stalk as a likely intermediate for fusion. The stalk is a semitoroidal structure that forms between the two apposed membranes and makes the contacting monolayers continuous, so that there is lipid mixing or hemifusion. The stalk is thermodynamically transient, and it expands radially leading to the formation of a fusion pore. While emphasizing such differences, we propose that PxB contacts are new species different than any of the fusion intermediates postulated thus far. First, as shown experimentally, the PxB-mediated contacts are thermodynamically stable, and the exchange of molecules present in the apposing monolayers through these contacts is selective. Another critical difference is that the stalk is a rate-limiting intermediate of membrane fusion, whereas the formation of PxB contacts is very rapid. Differences between stalk and peptide contact do not stop here. Formation of the stalk intermediate is influenced by the membrane lipid composition (Chernomordik & Zimmerberg, 1995). For example, micelle-forming lipids like lysophospholipids inhibit fusion (Chernomordik et al., 1993; Vogel et al., 1993), probably due to the fact that their positive spontaneous curvature is unfavorable for the formation of the negatively curved stalk (Kozlov & Markin, 1983). We have observed that the rate of lipid exchange through PxB-mediated contacts between DMPM vesicles is not affected by the presence of 4 mol % lysophospholipids, thus suggesting that the transfer through PxB contacts is relatively independent of the spontaneous curvature of the bulk lipid population.

Proteins as Agents for Direct Intermembrane Transfer of Phospholipids. The phenomenon described here has some broad implications with significant bearing on several cellular processes. Peptide-mediated selective intermembrane transfer or exchange of phospholipids without (hemi)fusion of membranes is implicated in several cellular processes. In eukaryotic cells, there are different intracellular membranes with different composition and function. Only a part of this diversity is due to asymmetric distribution of proteins and lipids (Krebs et al., 1979; Op den Kamp, 1979). This diversity is necessary for the viability of the cell, and, therefore, it must be regulated. Nevertheless, production of phospholipids and proteins is often centralized in few locations inside the cell: for example, most of the phospholipids are formed in the endoplasmic reticulum. Obviously, the cell must have an efficient mechanism for trafficking and sorting of proteins and lipids (Moreau & Cassagne, 1994) to maintain this diversity. Two nonexclusive processes have been implicated (Longmuir, 1987): specific phospholipid-transfer proteins (Dawidowicz, 1987; Wirtz, 1991) and

membrane flow either by diffusion through connections between membranes or by vesicle transport (Morre 1979). Vesicular membrane traffic and fusion between membranes is also implicated in many other physiological functions, i.e., intracellular membrane fusion events occur during movement of secretory material between the stacks of the Golgi apparatus, exocytosis of neurotransmitters and hormones, endocytosis, viral infection, cell division, fertilization, etc. For example, secretory vesicles are retrieved after exocytosis, without intermixing between vesicles and plasma membrane components; this is possibly due to the rapidity of the retrieval or to the absence of complete lipid fusion (Valtorta & Befenati, 1995; Bergeron, 1973).

To recapitulate, PxB-mediated molecular contacts are attractive prototype for selective intermembrane transfer of phospholipids. Specificity for the structure of the lipid head group is particularly interesting in this context because lipids sorted for head group could be tailored for the acylchains by acyltransferases present in specific organelles. The mechanisms conferring regulation and specificity for the intracellular transfer of phospholipids have not been articulated, yet it is widely accepted that proteins play a fundamental role in membrane fusion by fulfilling two basic requirements: cross-linking and destabilization of bilayers (White, 1992; Zimmerberg, 1993; Hoekstra, 1990). Specific proteins are involved in facilitation of merging of lipid membranes, target selection, and fusion regulation (Ferro-Novick & Jahn, 1994; Hughson, 1995; Schweizwer et al., 1995). We do not know yet which step in the membrane fusion cascade, if any, corresponds to the PxB contacts, nor do we know if a contact is a precursor or analog of the stalk.

ACKNOWLEDGMENT

We thank Drs. M. Bruch, L. V. Chernomordik, R. Epand, V. Markin, D. P. Siegel, and J. Vanderkooi for useful suggestions, stimulating discussions, and critical comments. M.K.J. acknowledges the hospitality of the Nehru Center (Bangalore), where some of this work was conceived.

REFERENCES

Apitz-Castro, R. J., Jain, M. K., & DeHaas, G. H. (1982) *Biochim. Biophys. Acta 688*, 349−356.
Berg, O. G., Yu, B.-Z., Rogers, J., & Jain, M. K. (1991) *Biochemistry 30*, 7283−7297.
Bergeron, J. J. M., Ehrenreich, J. H., Siekevitz, P., & Palade, E. (1973) *J. Cell. Biol. 59*, 73.
Cajal, Y., & Jain, M. K. (1996) *J. NIH Res.* (in press, May issue).
Cajal, Y., Berg, O. G., & Jain, M. K. (1995) *Biochem. Biophys. Res. Commun. 210*, 746−752.
Cajal, Y., Rogers, J., Berg, O. G., & Jain, M. K. (1996) *Biochemistry 35*, 299−308.
Chernomordik, L. V., & Zimmerberg, J. (1995) *Curr. Opin. Struct. Biol. 5*, 541−547.
Chernomordik, L. V., Vogel, S. S., Sokoloff, A., Onaran, H. O., Leikina, E. A., & Zimmerberg, J. (1993) *FEBS Lett. 318*, 71−76.
Craig, W. A., Turner, J. H., & Junin, C. M. (1974) *Infect. Immun. 10*, 287−292.
Dawidowicz, E. A. (1987) *Curr. Top. Membr. Transp. 29*, 175−202.
Ferro-Novick, S., & Jahn, R. (1994) *Nature 370*, 191−193.
Fields, R. (1972) *Methods Enzymol. 25*, 464−468.
Ghomashchi, F., Yu, B.-Z., Berg, O. G., Jain, M. J., & Gelb, M. H. (1991) *Biochemistry 30*, 7318−7329.
Hoekstra, D. (1990) *J. Bioenerg. Biomembr. 22*, 121−125.
Hughson, F. M. (1995) *Curr. Opin. Struct. Biol. 5*, 507−513.
Jain, M. K., & Berg, O. (1989) *Biochim. Biophys. Acta 1002*, 127−156.
Jain, M. K., Jahagirdar, D. V., VanLinde, M., Roelofsen, B., & Eibl, H. (1985) *Biochim. Biophys. Acta 818*, 356−364.
Jain, M. K., Rogers, J., Jahagirdar, D. V., Marecek, J. F., & Ramirez, F. (1986a) *Biochim. Biophys. Acta 860*, 435−447.
Jain, M. K., Maliwal, B. P., de Haas, G. H., & Slotboom, A. J. (1986b) *Biochim. Biophys. Acta 860*, 448−461.
Jain, M. K., Rogers, J., Marecek, J. F., Ramirez, F., & Eibl, H. (1986c) *Biochim. Biophys. Acta 860*, 462−474.
Jain, M. K., Yu, B.-Z., & Kozubek, A. (1989) *Biochim. Biophys. Acta 980*, 23−32.
Jain, M. K., Rogers, J., Berg, O., & Gelb, M. H. (1991) *Biochemistry 30*, 7340−7348.
Jain, M. K., Yu, B.-Z., Rogers, J., Gelb, M. H., Tsai, M. Hendrickson, E. K., & Hendrickson, S. (1992) *Biochemistry 32*, 7841−7847.
Jain, M. K., Gelb, M. H., Rogers, J., & Berg, O. G. (1995) *Methods Enzymol. 249*, 567−614.
Kozlov, M. M., & Markin, V. S. (1983) *Biofizika 28*, 255−261.
Krebs, J. J. R., Hauser, H., & Carafoli, E. (1979) *J. Biol. Chem. 254*, 5308−5316.
Kubesch, P., Boggs, J., Luciano, L., Maass, G., & Tümmler, B. (1987) *Biochemistry 26*, 2139−2149.
Longmuir, K. J. (1987) *Curr. Top. Membr. Transp. 29*, 129−174.
Lorey, E., Lami, H., & Laustrait, G. (1971) *Photochem. Photobiol. 14*, 411−421
Markin, V. S., Kozlov, M. M., & Borovjagin, V. L. (1984) *Gen. Physiol. Biophys. 5*, 361−370.
Moreau, P., & Cassagne, C. (1994) *Biochim. Biophys. Acta 1197*, 257−290.
Morre, D. J., Kartenbeck, J., & Franke, W. W. (1979) *Biochim. Biophys. Acta 559*, 71−152.
Op den Kamp, J. A. F. (1979) *Annu. Rev. Biochem. 48*, 47−71.
Schweizer, F. E., Betz, H., & Augustine, G. J. (1995) *Neuron 14*, 689−696.
Siegel, D. P. (1986a) *Biophys. J. 49*, 1155−1170.
Siegel, D. P. (1986b) *Biophys. J. 49*, 1171−1183.
Siegel, D. P. (1984) *Biophys. J. 45*, 399−420.
Siegel, D. P. (1993) *Biophys. J. 65*, 2124−2140.
Shinnar, A. E., Olsen, L., Shinnar, M., Reed, G., & Leig, J. S. (1993) *Biophys. J. 64*, 377.
Sixl, F., & Watts, A. (1985) *Biochemistry 24*, 7906−7910.
Storm, D. R., Rosenthal, K. S., & Swanson, P. E. (1977) *Annu. Rev. Biochem. 4*, 723−763.
Struck, D. K., Hoekstra, D., & Pagano, R. E. (1981) *Biochemistry 20*, 4093−4099.
Upreti, G. C., & Jain, M. K. (1980) *J. Membr. Biol. 55*, 113−123.
Valtorta, F., & Befenati, F. (1995) *Adv. Pharmacol. 32*, 505−557.
Verkleij, A. J., Mombers, C., Leunissen-Bijvelt, J., & Verbergaert, P. H. (1979) *Nature (London) 279*, 162−163.
Vogel, S. S., Leikina, E. A., & Chernomordik, L. V. (1993) *J. Biol. Chem. 268*, 25764−25768.
White, J. M. (1992) *Science 258*, 917−924.
Wirtz, K. W. A. (1991) *Annu. Rev. Biochem. 60*, 73−99.
Yu, B.-Z., Berg, O. G., & Jain, M. K. (1993) *Biochemistry 32*, 6485−6492.
Zidovetzki, R., Banerjee, U., Harrington, D. W., & Chan, S. I. (1988) *Biochemistry 27*, 5686−5692.
Zimmerberg, J., Vogel, S. S., & Chernomodik, L. V. (1993) *Annu. Rev. Biomol. Struct. 22*, 433−466.

BI952703C